**Noname manuscript No.**
(will be inserted by the editor)

# Modeling of dispersion-engineered all-chalcogenide step-index fiber for wideband supercontinuum generation in the mid-infrared

**M. R. Karim[1], Souvik Ghosh[2], M. M. Rahman[3], and B. M. A. Rahman[4]**

the date of receipt and acceptance should be inserted later

**Abstract** Mid-infrared region supercontinuum (SC) generation through designing broadband light sources recently attracts considerable attention in the field of nonlinear optics owing to their numerous applications in sensing and biological imaging. Broadband light sources designed based on different waveguiding structures adopted until today, the SC generation using optical step-index fiber is the prominent one due to its design and fabrication flexibility. In this study, a promising 5-cm-long SC source has been designed and modeled using a step-index fiber structure employing highly nonlinear chalcogenide (ChG) materials such as $As_2Se_3$ glass as a core and $Ge_{11.5}As_{24}Se_{64.5}$ glass for its outer cladding. Fiber structure is suitably modeled through its group-velocity dispersion optimization by varying core diameter. The optimized fiber structures are excited using a pump source having 170-fs pulses at 5.5 $\mu$m with a peak power of 10 kW. Initial all-normal dispersion excitation produces SC broadening up to 9.5 $\mu$m. Further study in a new optimization shows that spectral evolution can be expanded beyond 17 $\mu$m covering the wavelength from 3.2 $\mu$m to beyond 17 $\mu$m if the fiber structure is excited in the anomalous dispersion regime through a suitably tailored flat group-velocity dispersion curve with smaller in magnitude over a wide wavelength range. Such a promising SC source, which is designed based on typical step-index fiber principle using highly nonlinear ChG glass system, can be utilized in a variety of mid-infrared region applications.

M. R. Karim
E-mail: mrkarim@ciu.edu.bd

[1]Department of Electrical and Electronic Engineering, Chittagong Independent University, Chittagong, Bangladesh

[2,4]Department of Electrical and Electronic Engineering, City University of London, UK

[3]Department of Electronics and Communication Engineering, East West University, Dhaka, Bangladesh

**Keywords** Nonlinear optics and fibers · Dispersion · Glass and other amorphous materials · Supercontinuum generation

## 1 Introduction

Mid-infrared (MIR) supercontinuum (SC) generation has attracted a lot of researches interest due to its diverse applications in early cancer detection using optical biopsy [38], hyper-spectral infrared microscopy [7], multi-spectral tissue imaging [34], optical biosensing [29] and molecular fingerprint spectroscopy [33]. Recent reports on the broadband MIR SC sources used different nonlinear host materials, such as tellurite, fluoride and chalcogenide (ChG) glasses [42] to extend the SC spectra into MIR region. Among those, the ChG glasses are the prime choice for a broadband SC generation in the MIR region due to their higher optical nonlinearity and wider transparency ($\sim$ 25 $\mu$m) [1,37,8,28,10,17,43,3,23,21, 24,35].

Recently, several broadband SC spectral evolutions in the MIR using ChG fibers have been proposed [44,33,32,5,31,45,16,36,19,30,11]. Yu *et al.* [44] reported a MIR SC expansion spanning wavelength from 1.8 to 10 $\mu$m with a pulse width of 330-fs when pumped at 4 $\mu$m in a 11-cm-long ChG step-index fiber made from $Ge_{12}As_{24}Se_{64}$ as a core and $Ge_{12}As_{24}S_{64}$ as an outer cladding with an input peak power of 3 kW. Petersen *et al.* [33] reported a MIR region SC spectral broadening covering the wavelength from 1.4 $\mu$m to 13.3 $\mu$m with a 85-mm-long ChG step-index fiber using $As_{40}Se_{60}$ as the core and $Ge_{10}As_{23.5}Se_{66.6}$ glass for its outer cladding when pumped at 6.3 $\mu$m with pulses of 100-fs duration and an input peak power of 2.29 MW. The same group later reported a broadband MIR SC generation covering the wavelength from 1 to 11.5 $\mu$m with a high average output power using a tapered large-mode-area ChG $Ge_{11}As_{22}Se_{68}$ photonic crystal fiber (PCF) [32]. Cheng *et al.* [5] demonstrated a MIR SC generation spanning in the range of 2-15.1 $\mu$m in a 3-cm-long ChG step-index fiber using $As_2Se_3$ as the core and $AsSe_2$ as an outer cladding when pumped at 9.8 $\mu$m with a 170-fs duration pulses and a peak power of 2.89 MW. Ou *et al.* [31] reported a MIR SC spectral broadening up to 14 $\mu$m with a 20-cm-long ChG step-index fiber using $Ge_{15}Sb_{25}Se_{60}$ glass as the core and $Ge_{12}Sb_{20}Se_{65}$ glass the cladding when pumped at 6 $\mu$m with a 150-fs pulse duration and a peak power of 750 kW. Zhao *et al.* [45] reported a MIR SC spectra spanning up to 16 $\mu$m using a 14-cm-long step-index fiber made from Ge-Te-AgI glass when pumped at 7 $\mu$m with 150-fs duration pulses and a peak power of 77 MW. Hudson *et al.* [16] reported an ultrabroadband MIR SC spectral broadening spanning in the range of 1.8–9.5 $\mu$m using a $As_2Se_3/As_2S_3$ tapered fiber by launching 230-fs pulses with a pulse peak power of 4.2 kW. Wang *et al.* [42] demonstrated a MIR SC spectral evolution covering a wavelength range of 2–12.7 $\mu$m using a 12-cm-long step-index fiber using $As_2Se_3$ as the core and $As_2Se_2S$ as the outer cladding when pumped at 6.5 $\mu$m with a pulse of 150-fs duration and a peak power of 93 MW. Saini *et al.* [36] numerically demonstrated a MIR SC spectral evolution spanning in the range 2-15 $\mu$m in a 5-mm long triangular core graded index $As_2Se_3$ PCF when pumped at 4.1 $\mu$m with the largest peak power of 3.5 kW while Karim *et al.* [19] recently numerically demonstrated an ultrabroadband MIR SC generation spanning in the range 2.3–15 $\mu$m using a 10-mm-long all-ChG triangular core microstructured fiber (GeAsSe/GeAsS) when

**Table 1** Recent results on MIR SC spectral coverage obtained using ChG step-index fibers

| Materials (Core/Cladding) | Pump Wavelength | Spectral Coverage | Year [Ref.] |
|---|---|---|---|
| $Ge_{12}As_{24}Se_{64}/Ge_{12}As_{24}S_{64}$ | 4.0 $\mu$m | 1.8–10.0 $\mu$m | 2015 [44] |
| $As_{40}Se_{60}/Ge_{10}As_{23.5}Se_{66.6}$ | 6.3 $\mu$m | 1.4–13.3 $\mu$m | 2014 [33] |
| $As_2Se_3/AsSe_2$ | 9.8 $\mu$m | 2.0–15.1 $\mu$m | 2016 [5] |
| $Ge_{15}Sb_{25}Se_{60}/Ge_{12}Sb_{20}Se_{65}$ | 6.0 $\mu$m | 1.8–14.0 $\mu$m | 2016 [31] |
| $(Ge_{10}\text{-}Te_{43})_{90}\text{-}AgI_{10}/Ge_{10}Sb_{10}Se_{80}$ | 7.0 $\mu$m | 2.0–16.0 $\mu$m | 2017 [45] |
| $As_2Se_3/As_2Se_2S$ | 6.5 $\mu$m | 2.0–12.7 $\mu$m | 2018 [42] |
| $Ge_{20}Se_{60}Te_{20}/Ge_{20}Se_{70}Te_{10}$ | 7.7 $\mu$m | 2.0–14.0 $\mu$m | 2019 [24] |

pumped at 4 $\mu$m with a pulse duration of 100-fs and a low peak power of 3 kW. Due to inherent ability to integrate with different fluids, solids, and gases, recently hybrid/hollow-core band-gap guiding PCFs have attracted considerable attention as alternative to index guiding fibers [30]. Using a noble-gas-filled silica hollow-core anti-resonant hybrid PCF, Habib *et al.* [11] numerically demonstrated a SC generation in the range 1–4 $\mu$m through soliton-plasma interaction inside the fiber by employing a pump at 3 $\mu$m.

Table 1 presents recent results on MIR SC spectral coverage obtained using ChG step-index fibers made of different glass compositions. From table, it is apparent that the broadest MIR SC obtained with AsSe step-index fibers extends up to 15.1 $\mu$m [5] and spectral coverage further be extended up to 16 $\mu$m [45] by the same fiber structure made using modified ChG glass compositions (GeTe-AgI/GeSbSe). Further MIR spectral broadening can be achieved by using modified glass system having longer transmission window or by controlling the group-velocity dispersion (GVD) of the fiber geometry.

In this report, a promising 5-cm-long ChG step-index fiber structure constituted of $As_2Se_3$ glass for its core and $Ge_{11.5}As_{24}Se_{64.5}$ glass for its outer cladding is proposed for broadband SC generation in the MIR. Among the different compositions of ChG glasses, the proposed glass system posses optical transmission range up to 17.5 $\mu$m and 14 $\mu$m respectively having absorption coefficient ($\alpha$) of $1^{-\mathrm{cm}}$ [39]. Moreover, the similar thermo-optic coefficients [25] and high nonlinearity made the proposed glass system highly suitable for the step-index fiber fabrication. To achieve MIR SC spectral coverage up to the transparency limit of the proposed glass system, the fiber geometry is optimized by controlling GVD through the fiber structural parameter variation in such way that it is possible to achieve near-zero flattened GVD (wider region) for this design. The fiber is pumped with an input peak power of 10 kW at a wavelength of 5.5 $\mu$m. Five different ChG step-index fiber designs have been proposed and optimized within core diameter ranges between 6 and 9 $\mu$m and the SC spectral coverage at the output of each optimized design is discussed. Finally, one of the optimized design having core diameter of 7.5 $\mu$m shows that the SC spectral coverage at the output of the design (at a power level of -40 dB) could be exceeded the transmission limit (17.5 $\mu$m) of the proposed glass system. To the best of our knowledge, this could be the widest SC spectral coverage into the MIR by a typical step-index fiber design that is made of the ChG glass system proposed in this work.

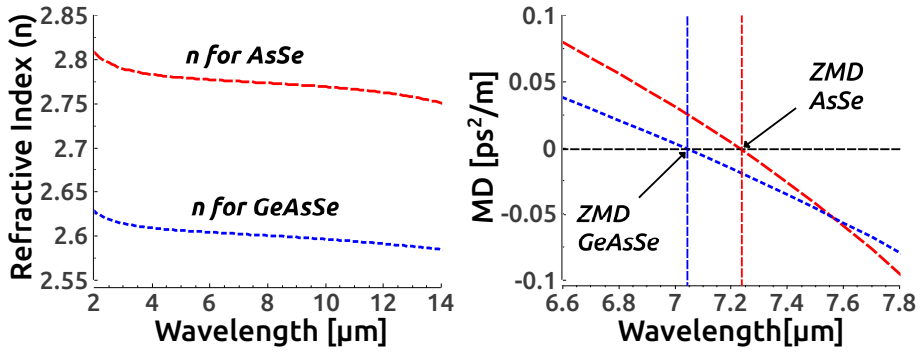


(a) (b)

**Fig. 1** (a) Refractive index distribution calculated over wide wavelength using Sellmeier equation for both AsSe and GeAsSe materials and (b) their corresponding material dispersions plotted to get their zero-material dispersion (ZMD) points.

## 2 Theory

A conventional step-index fiber design is followed with an $As_2Se_3$ glass as a core and $Ge_{11.5}As_{24}Se_{64.5}$ glass as an outer cladding medium. The Sellmeier equations from [41] and [27] are used to determine the wavelength dependent refractive index change and zero-material dispersion (ZMD) of $As_2Se_3$ and $Ge_{11.5}As_{24}Se_{64.5}$ ChG glasses, shown in Figs. 1(a) and 1(b), respectively.

The fiber is designed by varying its core diameter through a finite-element method (FEM) mode-solver using COMSOL Multiphysics. Figure 2 depicts the guided fundamental mode profiles ($H_x^{11}$) at two different wavelengths of 5.5 $\mu$m and 11 $\mu$m. The mode field profiles imply a good power confinement inside the proposed fiber. The fundamental mode ($H_x^{11}$) effective index $n_{\text{eff}}$ of the waveguides are obtained from the FEM simulation. Following that, the GVD as a function of

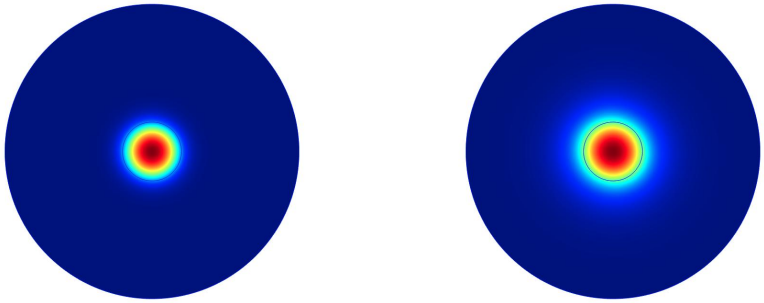

(a) (b)

**Fig. 2** Mode profiles of step-index fiber having core diameter of $d = 8$ $\mu$m at (a) 5.5 $\mu$m and (b) 11 $\mu$m for the for the fundamental mode of $H_x^{11}$.

wavelength are evaluated from the FEM obtained $n_{\text{eff}}$ data by using the dispersion equation [2]:

$$D(\lambda) = -\frac{\lambda}{c}\frac{d^2 n_{\text{eff}}}{d\lambda^2}, \tag{1}$$

where $\lambda$ and $c$ denote the wavelength in micrometer and the speed of light in the vacuum, respectively. Although the proposed fiber structure shows slight birefringent, it does not make any significant difference during GVD evaluations for the polarizations between quasi-TM ($H_x^{11}$) and quasi-TE ($H_y^{11}$) modes.

A sufficiently intense pulse injection into the optical waveguide induces several nonlinear effects, such as self-phase modulation (SPM), Raman scattering, and dispersive wave (DW). The interplay between the induced nonlinear effects and the GVD inside the optical waveguide generates a continuous spectral broadening (known as SC) as output. To study the generation of a SC through launching an ultra-short optical pulse into the proposed ChG step-index fiber, the generalized nonlinear Schrödinger equation (GNLSE) can be solved by the split-step Fourier method, a widely employed method for obtaining a pulse evolution inside the waveguiding structure [2,6]:

$$\frac{\partial}{\partial z}A(z,T) + \frac{\alpha}{2}A - \sum_{m\geq 2}^{16}\frac{i^{m+1}}{m!}\beta_m\frac{\partial^m A}{\partial T^m} = i\gamma\left(1+\frac{i}{\omega_0}\frac{\partial}{\partial T}\right) \times \left(A(z,T)\int_{-\infty}^{\infty} R(T) \mid A(z,T-T') \mid^2 dT'\right), \tag{2}$$

The left and right hand sides of Eq. (2) express the linear and the nonlinear effects acting while optical pulses propagating inside the fiber. $A(z,T)$ is the electric field envelop which moves at the group velocity of $1/\beta_1$ ($T = t - \beta_1 z$). $\beta_m$ ($m \geq 2$) expresses the $m^{\text{th}}$ order dispersion parameter and $\omega_0$ is the center angular frequency of the pump source. The nonlinear coefficient is defined as $\gamma = n_2\omega_0/(cA_{\text{eff}})$, where $A_{\text{eff}}$ and $n_2$ represent the mode-effective area and the nonlinear refractive index parameter, respectively. $\alpha$ is denoted the fiber transmission loss.

Intrapulse Raman scattering plays a significant role during the SC evolution inside the fiber. It includes both the delayed Raman contribution ($h_{\text{R}}$) and instantaneous electronic contribution ($f_{\text{R}}$) through the following response function [2]:

$$R(t) = (1 - f_{\text{R}})\delta(t) + f_{\text{R}}h_{\text{R(t)}}, \tag{3}$$

with the Raman contribution having the form

$$h_{\text{R(t)}} = \frac{\tau_1^2 + \tau_2^2}{\tau_1\tau_2^2}\exp\left(-\frac{t}{\tau_2}\right)\sin\left(\frac{t}{\tau_1}\right). \tag{4}$$

In this case, the $f_{\text{R}}$ value for $As_2Se_3$ glass is considered to be 0.148. $\tau_1$ and $\tau_2$ are considered to be 23-fs and 164.5-fs, respectively [26].

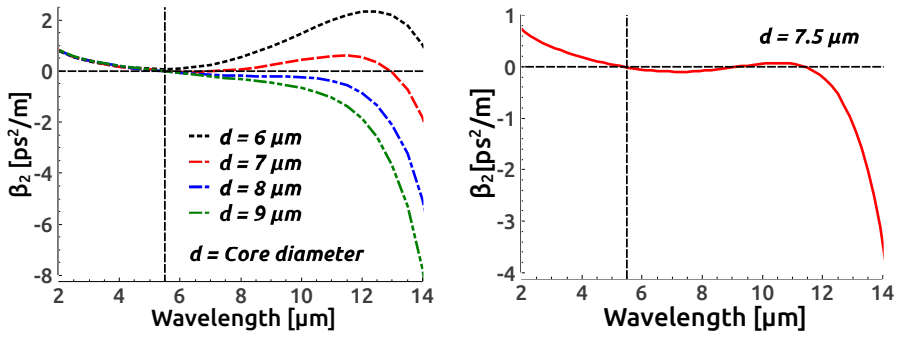


(a) (b)

**Fig. 3** GVD curves for the $As_2Se_3$ step-index fiber optimized for pumping at 5.5 $\mu$m by varying fiber core diameter ($d$) between 6 $\mu$m and 9 $\mu$m. Vertical dashed line indicates pump wavelength.

## 3 Numerical Results

For an efficient SC generation and a broadband SC expansion in the long wavelength side of the MIR, the optical fiber needs to be driven with a low GVD in the vicinity to the zero-dispersion wavelength (ZDW) with an wide but flat anomalous dispersion region GVD curve [6]. An employment of the pump source excitation into the optimized waveguide in long wavelength pushes the long wavelength edge of the SC spectra far into the MIR. It also needs to be followed that the pump wavelength must be vicinity to the ZDW of the GVD curve. Depending on the practical availability of a pump source in the long wavelength region, a fiber for an wideband SC generation is engineered by varying its core diameter between 6 $\mu$m and 9 $\mu$m. Using a difference frequency generator, Cheng *et al.* [5] has reported a tunable pump source in the range 2.4–11 $\mu$m with a pulse width of 170-fs duration and a repetition rate of 1 kHz. Considering this tunning wavelength range, a fiber structure is initially designed with a core diameter of 6 $\mu$m whose GVD curve (dotted-black) is shown in Fig. 3(a). The main underline point is that this GVD

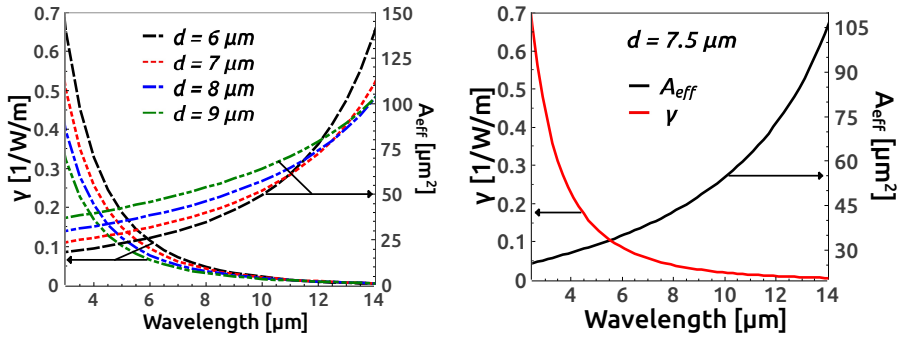


(a) (b)

**Fig. 4** Wavelength dependent $A_{\text{eff}}$ of proposed step-index fiber with different core diameter variations and their corresponding nonlinear parameters are evaluated.

curve purely remains in normal dispersion region until 14 $\mu$m. The minimum GVD ($\beta_2$ = 0.077 ps$^2$/m) is obtained at a wavelength of 5.5 $\mu$m. To optimize a design with an anomalous dispersion region in the GVD curve, the fiber core diameter is increased to 7 $\mu$m and the tailored dispersion curve for this design is shown in Fig. 3(a) by a red dashed line. This design exhibits a small anomalous dispersion between 6 and 7 $\mu$m. On the other hand, the GVD curve remains in the normal dispersion between 7 and 13 $\mu$m and later it sharply enters into the anomalous dispersion region again beyond 13 $\mu$m. To achieve a wide anomalous dispersion, next fiber structure is tailored by increasing its diameter to 7.5 $\mu$m which results increasing of anomalous GVD region up to 9.3 $\mu$m. Figure 3(b) shows a GVD curve for this design having small magnitude but nearly flat GVD over wide wavelength range. Three ZDWs are appeared on this GVD curve and a steep GVD edge is observed in the long wavelength side after 14 $\mu$m wavelength. The minimum anomalous GVD, $\beta_2$ = -0.013 ps$^2$/m, in this case, is obtained at 5.5 $\mu$m wavelength. Two more designs are further modeled by increasing fiber core diameter at 8 and 9 $\mu$m. The GVD curves for these designs are shown in Fig. 3(a) with blue dashed-dotted and green dashed-double dotted lines, respectively. The blue curve shows a nearly flat and very low GVD values until 11 $\mu$m and obtains a minimum anomalous GVD ($\beta_2$ = -0.019 ps$^2$/m) at 5.5 $\mu$m. It is achieved by a simple step-index fiber design with a core diameter of 8 $\mu$m. On the other hand, a higher slope GVD curve in the long wavelength side with a minimum anomalous GVD ($\beta_2$ = -0.021 ps$^2$/m) at 5.5 $\mu$m is obtained for a fiber with a core diameter of 9 $\mu$m. As the minimum anomalous GVD is observed for last three designs at 5.5 $\mu$m, the pump source is tunned at 5.5 $\mu$m wavelength to excite the all proposed designs during numerical simulations. It is worth noting in Fig. 1(b) that the zero-material dispersion (ZMD) for both core and cladding materials is located at around 7 $\mu$m and it is difficult to achieve an anomalous dispersion region starting a ZDW before 5.5 $\mu$m owing to have a high material dispersion of ChG glasses chosen in these step-index fiber designs.

In order to predict an ultrawideband MIR SC generation by the proposed step-index fiber, numerical simulations are carried out by solving the GNLSE Eq. (2) using symmetric split-step Fourier method through an in-house MATLAB code. The numerical simulation consists of $2^{17}$ grid points with minimum temporal resolution of 9.2-fs at the pump wavelength so that the time window can readily accommodate extreme spectral broadening by avoiding negative frequency generation. The number of steps are taken as 100,000 with a step size of 200 nm. The spurious SC spectral evolution at the output is suppressed by considering higher-order dispersion terms up to 16$^{\text{th}}$ order ($\beta_{16}$) during all numerical simulations [22]. The mode-effective areas of the proposed fibers are calculated using the FEM mode-solver and their corresponding nonlinear coefficients are evaluated by considering the nonlinear refractive index, $n_2 = 1.1 \times 10^{-17}$ m$^2$/W [5]. Figure 4 shows the dispersion of mode effective area and corresponding nonlinear coefficient. An average linear propagation loss of 0.65 dB/cm is considered for a $As_2Se_3$ glass fiber at a wavelength of 10.6 $\mu$m, reported by Shiryaev *et al.* [39]. Here, the assumed absorption loss is more than that reported by Wang *et al.* [42] in their proposed 12-cm-long $As_2Se_3$ step-index fiber design for MIR region SC generation. The aforementioned work reports the average loss to be approximately 4 dB/m between 2.5 $\mu$m and 12 $\mu$m with two strong peaks of As-O and Se-O lo-

cated around at 8.2 $\mu$m and 10.5 $\mu$m, respectively. Typically, the transmission loss against wavelength for $As_2Se_3$ increases rapidly above a wavelength of 12 $\mu$m.

Initially, simulations are performed for the all-normal dispersion SC spectral evolution in the proposed fiber whose corresponding GVD curve (dotted-balck) is shown in Fig. 3(a). Mode effective area, $A_{\text{eff}}$ and its corresponding nonlinear coefficient, $\gamma$ at the pump wavelength of 5.5 $\mu$m are calculated as 24.41 $\mu m^2$ and 0.15 /W/m, respectively. A sech pulse of 170-fs duration is launched into the fiber geometry with an input peak power of 10 kW. Figure 5(a) illustrates the predicted SC spectrum (solid-black line) at the optimized fiber output. A smooth and flat SC bandwidth up to 6 $\mu$m could be realized by this design covering the MIR spectral region from 3.5 $\mu$m to 9.5 $\mu$m. Since the tailored GVD curve for this fiber geometry (with a core diameter of 6 $\mu$m) remains in the all-normal dispersion regime, a narrowband SC expansion is realized owing to the suppression of solitonic fission inside the fiber. Further, it is worth noting that a flat SC spectrum with uniform spectral power distribution over the entire output spectra is possible if the waveguiding geometries are pumped in the all-normal dispersion regime [18].

Next simulation is carried out using the red-dashed GVD curve in Fig. 3(a) to obtain a further MIR SC expansion in the long wavelength side. This dispersion

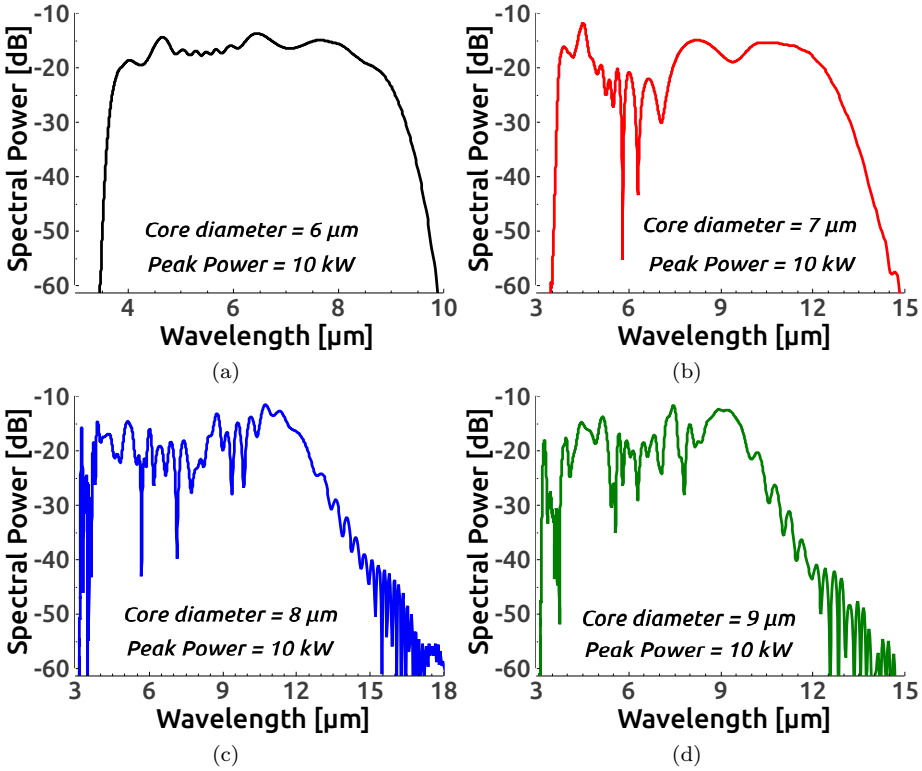


**Fig. 5** Output SC spectra for the step-index fiber having (a) $d = 6$ $\mu$m, (b) $d = 7$ $\mu$m, (c) $d = 8$ $\mu$m, and (d) $d = 9$ $\mu$m for the largest input pump peak power of 10 kW employing pump at 5.5 $\mu$m. Spectra obtained in (a), (b) and (c), (d) are in normal and anomalous dispersion region pumping, respectively.

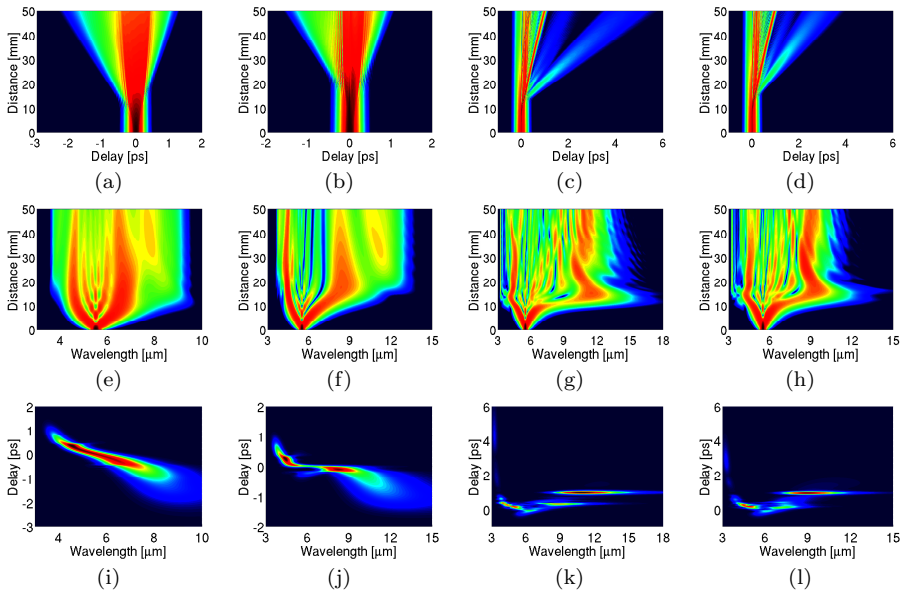


**Fig. 6** Temporal, Spectral and Spectrogram are obtained using pump at 5.5 $\mu$m with the largest input pump peak power of 10 kW. Column 1 to 4 correspond to the spectra shown by the (a), (b), (c) and (d) of Fig. 5, respectively.

curve has been tailored for the fiber structure having core diameter of 7 $\mu$m. $A_{\text{eff}}$ and $\gamma$ of the fiber at the pump wavelength are evaluated as 30.17 $\mu$m$^2$ and 0.12 /W/m, respectively. A rigorous study shows that the SC broadening could able to be achieved with a bandwidth more than 10 $\mu$m by this design. Figure 5(b) shows the MIR spanning from 3.6 $\mu$m to 13.7 $\mu$m at -30 dB level from the peak. Although a small anomalous dispersion region is appeared in this design, the SC spectrum does not broaden significantly at the fiber output due to soliton fission suppression because of normal dispersion pumping excitation.

The SC spectrum further can be widened on both sides by employing a pump in the anomalous dispersion regime. The GVD curve (blue dotted-dashed line) in Fig. 3(a) is tailored for fiber structure having a core diameter of 8 $\mu$m. $A_{\text{eff}}$ and $\gamma$ at the pump wavelength for this fiber structure are calculated as 36.79 $\mu$m$^2$ and 0.096 /W/m, respectively. The anomalous GVD region for this design is started before 5.5 $\mu$m. So, by using a pump at 5.5 $\mu$m with a peak power of 10 kW the SC spectrum can be expanded in both sides from 3 $\mu$m to 14.5 $\mu$m, shown in Fig. 5(c). The spectral expansion does not extend beyond 14.5 $\mu$m due to the sharp increment of GVD values after the wavelength of 14 $\mu$m. Raising fiber core diameter to 9 $\mu$m, $A_{\text{eff}}$ and $\gamma$ are obtained as 44.24 $\mu$m$^2$ and 0.021 /W/m, respectively. Further increment in core diameter does not enhance the spectral broadening, instead reduces the output bandwidth. It can be seen in Fig. 5(d), which shows the SC spectral evolution covers the wavelength range 3.2–12 $\mu$m at the fiber output. The GVD curve for this design exhibits a rapid increment with a higher slope before 14 $\mu$m which results in a reduced SC bandwidth at the fiber output.

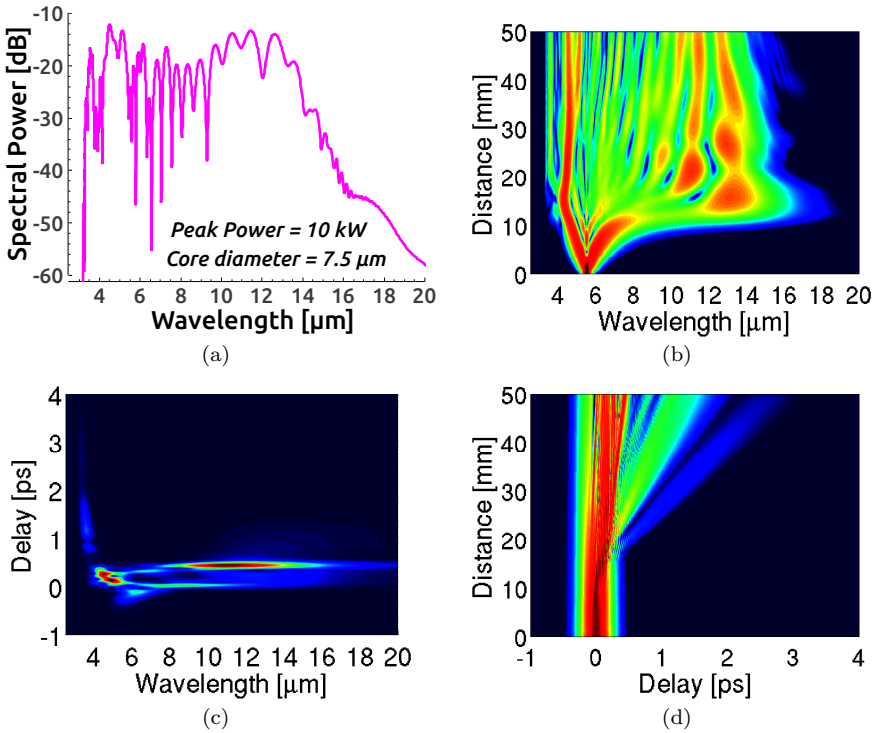


**Fig. 7** (a) SC spectrum; (b) Temporal density; (c) Spectral density; and (d) Spectrogram at the output of a step-index fiber with a core diameter, $d = 7.5$ $\mu$m for an input pump peak power of 10 kW while employing pump at 5.5 $\mu$m.

The SC spectra are not broadened sufficiently by the four fiber designs shown in the earlier analysis. To get an optimum design with sufficient SC spectral broadening at the fiber output, one more fiber structure is engineered by considering the core diameter between 7 and 8 $\mu$m whose GVD curve is shown in Fig. 3(b). The calculated values of $A_{\text{eff}}$ and their corresponding values of $\gamma$ for this design are shown in Fig. 4(b) and the estimated values of these two parameters at pump wavelength are 33.38 $\mu$m$^2$ and 0.11 /W/m, respectively. Keeping all other parameters are same as used in earlier designs, the numerical simulation is carried out to see the SC broadening at the fiber output. Figure 7 shows the SC evolution covering the wavelength range in the MIR from 3.2 $\mu$m to beyond 17 $\mu$m with a bandwidth of around 14 $\mu$m estimated at a power level of -40 dB from the peak which is higher than the bandwidth obtained by all the proposed designs discussed earlier. Even at high power level (at -10 dB from the peak), it can be observed from Fig. 7(a) that the SC spectrum extends up to 14 $\mu$m. Thanks to the ChG glass system that we have chosen with index contrast shown in Fig. 1(a) through which we are able to optimize a fiber geometry for ultrawide SC spectral coverage by controlling its GVD. Thus, the widest SC spectral coverage, as per as we know from the best of our knowledge, is observed through numerical simulation by a typical step-index fiber structure with a core diameter of 7.5 $\mu$m among the five geometries proposed in this work.

The SC spectral broadening in the all-normal dispersion pumping is initially dominated by SPM and later by optical wave breaking (OWB) [13,14,9,12,4,40, 15,20]. As the pump falls in the normal GVD region, the SC spectra is broadened in the absence of soliton fission process inside the fiber. After launching an ultra-short optical pulse into the fiber, initially, the SC spectra inside the fiber is symmetrically expanded by SPM. This in turn makes the longer wavelength faster compared to the shorter components. Therefore, an overlap of different frequency components can be observed here. In the temporal regime, the overlap of these pulse components leads to produce new frequency components which result in two side-lobes (OWBs) in either side of the central spectrum. This can be observed clearly from the all-normal dispersion spectral densities and spectrograms, illustrated in Figs. 6(e)-6(f) and Figs. 6(i)-6(j), respectively.

During anomalous dispersion pumping excitation, the pulse dynamics inside the optical fibers is mainly dominated by solitonic propagation. The pulse spectral evolution in Fig. 6(a) – (l) illustrate the SC evolution along the 5-cm long fiber geometry driven by a pump wavelength of 5.5 $\mu$m. Initially, owing to SPM, soliton undergoes temporal compression which results in a primary SC spectral broadening at the fiber output. These soliton orders can be calculated as, $N = \sqrt{L_{\mathrm{D}}/L_{\mathrm{NL}}}$, where $L_{\mathrm{D}}$ and $L_{\mathrm{NL}}$ are the dispersion and nonlinear lengths, respectively. During pulse propagation through the fiber, optical pulses are perturbed and encountered by higher-order dispersion and Raman scattering. This in turn breaks the pulse envelop into $N$ number of fundamental solitions by solition fission processes. Soliton fission occurs around 1.4 cm fiber length having core diameters of 7.5, 8 and 9 $\mu$m, shown in Figs. 6(c), 6(d), and 7(b), respectively. The fission process produces 20, 18 and 27 fundamental solitons for the last three designs, respectively. The fundamental solitons red shifted continuously due to the Raman scattering which yields an expansion of the SC spectra in the long wavelength side. Considering the presence of higher-order dispersion parameters, a blue shifted resonant narrowband DW is induced at around 3 $\mu$m for last three designs before the first ZDW of the GVD curve, shown in Figs. 6(g), 6(h) and 7(c), respectively.

## 4 Conclusion

In this work, we have investigated a broadband SC generation in the MIR using a 5-cm-long dispersion-engineered all ChG step-index fiber. Numerical analysis has been carried out for designing a suitable step-index fiber structure by varying fiber core diameter between 6 $\mu$m and 9 $\mu$m. GVD analysis reveals that it is not possible to design a fiber using a core diameter below 7 $\mu$m for pumping at 5.5 $\mu$m in the anomalous dispersion regime. Fiber core diameter below 7 $\mu$m produces an all-normal dispersion fiber design. Using a core diameter at 6 $\mu$m, all-normal dispersion SC can be generated up to 9.5 $\mu$m with a peak power of 10 kW. Due to soliton fission suppression in the all-normal dispersion pumping, a flat top SC spectral evolution can be generated over the entire bandwidth at the fiber output. The SC broadening can be enhanced in the all-normal dispersion pumping by increasing core diameter to 7 $\mu$m. In this case, spectral broadening up to 13.7 $\mu$m could be achieved. To increase bandwidth further in the long wavelength side, a step-index fiber is designed for pumping in the anomalous GVD region by increasing core diameter to 7.5 $\mu$m. Simulation result shows that the SC spectrum can be

broadened by this design beyond 17 $\mu$m which is equivalent to transmission limit of the ChG glass system proposed. Anomalous dispersion pumping also broadens the spectrum towards the short wavelength side as well. Thus, the SC output can cover the MIR wavelength range from 3.2 $\mu$m to beyond the transparency limit of the proposed glass system with a fiber core diameter of 7.5 $\mu$m and an input peak power of 10 kW and to the best of our knowledge, this could be the broadest SC spectral coverage into the MIR by a conventional step-index fiber design. Further increasing fiber core diameter does not enhance the spectral broadening instead reduces the bandwidth at the fiber output due to a higher GVD slop. Thus, the proposed structure, which is designed and modeled based on step-index fiber principle, can be suitable for an efficient broadband SC spectral evolution in the MIR and may be used for a variety of applications in the important areas of MIR region sensing and biological imaging.

## References


1. Aggarwal, I.D., Sanghera, J.S.: Development and applications of chalcogenide glass optical fibers at nrl. J. Optoelectron. Adv. Mater **4**(3), 665–678 (2002)
2. Agrawal, G.P.: Nonlinear fiber optics. In: Nonlinear Science at the Dawn of the 21st Century, pp. 195–211. Springer (2000)
3. Al-Kadry, A., El Amraoui, M., Messaddeq, Y., Rochette, M.: Two octaves mid-infrared supercontinuum generation in $As_2Se_3$ microwires. Optics Express **22**(25), 31,131–31,137 (2014)
4. B. Siwicki M. klimczak, R.S., Buczynski, R.: Supercontinuum generation enhancement in all-solid all-normal dispersion soft glass photonic crystal fiber pumped at 1550 nm. Optical Fiber Technology **25**, 64–71 (2015)
5. Cheng, T., Nagasaka, K., Tuan, T.H., Xue, X., Matsumoto, M., Tezuka, H., Suzuki, T., Ohishi, Y.: Mid-infrared supercontinuum generation spanning 2.0 to 15.1 $\mu$m in a chalcogenide step-index fiber. Optics letters **41**(9), 2117–2120 (2016)
6. Dudley, J.M., Genty, G., Coen, S.: Supercontinuum generation in photonic crystal fiber. Reviews of modern physics **78**(4), 1135–1184 (2006)
7. Dupont, S., Petersen, C., Thøgersen, J., Agger, C., Bang, O., Keiding, S.R.: Ir microscopy utilizing intense supercontinuum light source. Optics Express **20**(5), 4887–4892 (2012)
8. Eggleton, B.J., Luther-Davies, B., Richardson, K.: Chalcogenide photonics. Nature photonics **5**(3), 141 (2011)
9. Finot, C., Kibler, B., Provost, L., Wabnitz, S.: Beneficial impact of wave-breaking for coherent continuum formation in normally dispersive nonlinear fibers. J. Opt. Soc. Am. B **25**(11), 1938–1948 (2008). DOI 10.1364/JOSAB.25.001938
10. Gai, X., Han, T., Prasad, A., Madden, S., Choi, D.Y., Wang, R., Bulla, D., Luther-Davies, B.: Progress in optical waveguides fabricated from chalcogenide glasses. Optics express **18**(25), 26,635–26,646 (2010)
11. Habib, M.S., Markos, C., Bang, O., Bache, M.: Soliton-plasma nonlinear dynamics in mid-ir gas-filled hollow-core fibers. Optics letters **42**(11), 2232–2235 (2017)
12. Hartung, A., Heidt, A.M., Bartelt, H.: Design of all-normal dispersion microstructured optical fibers for pulse-preserving supercontinuum generation. Opt. Express **19**(8), 7742–7749 (2011). DOI 10.1364/OE.19.007742
13. Heidt, A.M.: Pulse preserving flat-top supercontinuum generation in all-normal dispersion photonic crystal fibers. JOSA B **27**(3), 550–559 (2010)
14. Heidt, A.M., Hartung, A., Bosman, G.W., Krok, P., Rohwer, E.G., Schwoerer, H., Bartelt, H.: Coherent octave spanning near-infrared and visible supercontinuum generation in all-normal dispersion photonic crystal fibers. Optics express **19**(4), 3775–3787 (2011)
15. Hooper, L.E., Mosley, P.J., Muir, A.C., Wadsworth, W.J., Knight, J.C.: Coherent supercontinuum generation in photonic crystal fiber with all-normal group velocity dispersion. Optics express **19**(6), 4902–4907 (2011)
16. Hudson, D.D., Antipov, S., Li, L., Alamgir, I., Hu, T., El Amraoui, M., Messaddeq, Y., Rochette, M., Jackson, S.D., Fuerbach, A.: Toward all-fiber supercontinuum spanning the mid-infrared. Optica **4**(10), 1163–1166 (2017)

17. Hudson, D.D., Mägi, E.C., Judge, A.C., Dekker, S.A., Eggleton, B.J.: Highly nonlinear chalcogenide glass micro/nanofiber devices: Design, theory, and octave-spanning spectral generation. Optics Communications **285**(23), 4660–4669 (2012)
18. Karim, M., Ahmad, H., Rahman, B.: All-normal dispersion chalcogenide pcf for ultraflat mid-infrared supercontinuum generation. IEEE Photonics Technology Letters **29**(21), 1792–1795 (2017)
19. Karim, M., Ahmad, H., Rahman, B.: Design and modeling of dispersion-engineered all-chalcogenide triangular-core fiber for mid-infrared-region supercontinuum generation. JOSA B **35**(2), 266–275 (2018)
20. Karim, M., Ahmad, H., Rahman, B.A.: All-normal-dispersion chalcogenide waveguides for ultraflat supercontinuum generation in the mid-infrared region. IEEE Journal of Quantum Electronics **53**(2), 1–6 (2017)
21. Karim, M., Rahman, B., Azabi, Y., Agrawal, A., Agrawal, G.P.: Ultrabroadband mid-infrared supercontinuum generation through dispersion engineering of chalcogenide microstructured fibers. JOSA B **32**(11), 2343–2351 (2015)
22. Karim, M.R., Ahmad, H., Ghosh, S., Rahman, B.: Mid-infrared supercontinuum generation using $As_2Se_3$ photonic crystal fiber and the impact of higher-order dispersion parameters on its supercontinuum bandwidth. Optical Fiber Technology **45**, 255–266 (2018)
23. Kubat, I., Agger, C.S., Møller, U., Seddon, A.B., Tang, Z., Sujecki, S., Benson, T.M., Furniss, D., Lamrini, S., Scholle, K., et al.: Mid-infrared supercontinuum generation to 12.5 $\mu$m in large na chalcogenide step-index fibres pumped at 4.5 $\mu$m. Optics express **22**(16), 19,169–19,182 (2014)
24. Lemière, A., Désévédavy, F., Mathey, P., Froidevaux, P., Gadret, G., Jules, J.C., Aquilina, C., Kibler, B., Béjot, P., Billard, F., et al.: Mid-infrared supercontinuum generation from 2 to 14 $\mu$m in arsenic-and antimony-free chalcogenide glass fibers. JOSA B **36**(2), A183–A192 (2019)
25. Lian, Z.G., Li, Q.Q., Furniss, D., Benson, T.M., Seddon, A.B.: Solid microstructured chalcogenide glass optical fibers for the near-and mid-infrared spectral regions. IEEE Photonics Technology Letters **21**(24), 1804–1806 (2009)
26. Liu, L., Cheng, T., Nagasaka, K., Tong, H., Qin, G., Suzuki, T., Ohishi, Y.: Coherent mid-infrared supercontinuum generation in all-solid chalcogenide microstructured fibers with all-normal dispersion. Optics letters **41**(2), 392–395 (2016)
27. Ma, P., Choi, D.Y., Yu, Y., Gai, X., Yang, Z., Debbarma, S., Madden, S., Luther-Davies, B.: Low-loss chalcogenide waveguides for chemical sensing in the mid-infrared. Optics express **21**(24), 29,927–29,937 (2013)
28. Mägi, E.C., Fu, L., Nguyen, H.C., Lamont, M., Yeom, D., Eggleton, B.: Enhanced kerr nonlinearity in sub-wavelength diameter $As_2Se_3$ chalcogenide fiber tapers. Optics Express **15**(16), 10,324–10,329 (2007)
29. Markos, C., Bang, O.: Nonlinear label-free biosensing with high sensitivity using $As_2S_3$ chalcogenide tapered fiber. Journal of Lightwave Technology **33**(13), 2892–2898 (2015)
30. Markos, C., Travers, J.C., Abdolvand, A., Eggleton, B.J., Bang, O.: Hybrid photonic-crystal fiber. Reviews of Modern Physics **89**(4), 045,003 (2017)
31. Ou, H., Dai, S., Zhang, P., Liu, Z., Wang, X., Chen, F., Xu, H., Luo, B., Huang, Y., Wang, R.: Ultrabroad supercontinuum generated from a highly nonlinear Ge–Sb–Se fiber. Optics letters **41**(14), 3201–3204 (2016)
32. Petersen, C.R., Engelsholm, R.D., Markos, C., Brilland, L., Caillaud, C., Trolès, J., Bang, O.: Increased mid-infrared supercontinuum bandwidth and average power by tapering large-mode-area chalcogenide photonic crystal fibers. Optics express **25**(13), 15,336–15,348 (2017)
33. Petersen, C.R., Møller, U., Kubat, I., Zhou, B., Dupont, S., Ramsay, J., Benson, T., Sujecki, S., Abdel-Moneim, N., Tang, Z., et al.: Mid-infrared supercontinuum covering the 1.4–13.3 $\mu$m molecular fingerprint region using ultra-high na chalcogenide step-index fibre. Nature Photonics **8**(11), 830 (2014)
34. Petersen, C.R., Prtljaga, N., Farries, M., Ward, J., Napier, B., Lloyd, G.R., Nallala, J., Stone, N., Bang, O.: Mid-infrared multispectral tissue imaging using a chalcogenide fiber supercontinuum source. Optics letters **43**(5), 999–1002 (2018)
35. Saghaei, H., Ebnali-Heidari, M., Moravvej-Farshi, M.K.: Midinfrared supercontinuum generation via $As_2Se_3$ chalcogenide photonic crystal fibers. Applied optics **54**(8), 2072–2079 (2015)
36. Saini, T.S., Kumar, A., Sinha, R.K.: Broadband mid-infrared supercontinuum spectra spanning 2–15 $\mu$m using $As_2Se_3$ chalcogenide glass triangular-core graded-index photonic crystal fiber. Journal of lightwave technology **33**(18), 3914–3920 (2015)

37. Sanghera, J., Florea, C., Shaw, L., Pureza, P., Nguyen, V., Bashkansky, M., Dutton, Z., Aggarwal, I.: Non-linear properties of chalcogenide glasses and fibers. Journal of Non-Crystalline Solids **354**(2-9), 462–467 (2008)
38. Seddon, A.B., Napier, B., Lindsay, I., Lamrini, S., Moselund, P.M., Stone, N., Bang, O.: Mid-infrared spectroscopy/bioimaging: Moving toward mir optical biopsy. Laser Focus World **52**(2), 50–53 (2016)
39. Shiryaev, V., Churbanov, M.: Trends and prospects for development of chalcogenide fibers for mid-infrared transmission. Journal of Non-Crystalline Solids **377**, 225–230 (2013)
40. Stepniewski, G., Klimczak, M., Bookey, H., Siwicki, B., Pysz, D., Stepien, R., Kar, A., Waddie, A., Taghizadeh, M., Buczynski, R.: Broadband supercontinuum generation in normal dispersion all-solid photonic crystal fiber pumped near 1300 nm. Laser Physics Letters **11**(5), 055,103 (2014)
41. Ung, B., Skorobogatiy, M.: Chalcogenide microporous fibers for linear and nonlinear applications in the mid-infrared. Optics express **18**(8), 8647–8659 (2010)
42. Wang, Y., Dai, S., Han, X., Zhang, P., Liu, Y., Wang, X., Sun, S.: Broadband mid-infrared supercontinuum generation in novel $As_2Se_3$-$As_2Se_2S$ step-index fibers. Optics Communications **410**, 410–415 (2018)
43. Wei, C., Zhu, X., Norwood, R.A., Song, F., Peyghambarian, N.: Numerical investigation on high power mid-infrared supercontinuum fiber lasers pumped at 3 $\mu$m. Optics express **21**(24), 29,488–29,504 (2013)
44. Yu, Y., Zhang, B., Gai, X., Zhai, C., Qi, S., Guo, W., Yang, Z., Wang, R., Choi, D.Y., Madden, S., et al.: 1.8-10 $\mu$m mid-infrared supercontinuum generated in a step-index chalcogenide fiber using low peak pump power. Optics letters **40**(6), 1081–1084 (2015)
45. Zhao, Z., Wu, B., Wang, X., Pan, Z., Liu, Z., Zhang, P., Shen, X., Nie, Q., Dai, S., Wang, R.: Mid-infrared supercontinuum covering 2.0–16 $\mu$m in a low-loss telluride single-mode fiber. Laser & Photonics Reviews **11**(2), 1700,005 (2017)